Discrete peaks in above-threshold double-ionization spectra

M. Lein,[1,2] E. K. U. Gross,[2] and V. Engel[1]
[1]*Institut für Physikalische Chemie, Am Hubland, 97074 Würzburg, Germany*
[2]*Institut für Theoretische Physik, Am Hubland, 97074 Würzburg, Germany*
(Received 20 October 2000; published 2 July 2001)

Quantum-mechanical calculations of multiphoton double ionization by intense laser pulses show that the total-kinetic-energy spectrum of the photoelectrons consists of peaks separated by the photon energy, analogous to ordinary above-threshold ionization. Related structures appear in the two-electron and in the recoil-ion momentum distribution. We propose a method to extract the total-kinetic-energy spectrum from the experimental recoil-ion spectrum.

DOI: 10.1103/PhysRevA.64.023406 PACS number(s): 32.80.Rm, 31.70.Hq, 32.80.Fb

When an atom is exposed to intense laser radiation, multiphoton ionization can proceed via absorption of more photons than required to exceed the ionization threshold. This effect, known as above-threshold ionization (ATI), was first observed over 20 years ago [1]. In the photoelectron energy spectra, ATI typically manifests itself as peaks that are separated by the photon energy. Detailed studies have been devoted to the structure of the ATI spectra [2]. In the past decade, the observation of such new effects as the plateau in ATI spectra [3] and the unexpected ellipticity dependence [4] gave rise to continuing interest in the phenomenon. As far as the numerical treatment is concerned, photoelectron spectra have been calculated accurately and efficiently [5] within the single-active electron approximation.

Laser-induced double ionization has been another topic of great interest in the past few years, triggered by the discovery of unexpectedly large double-ionization rates [6,7] that could not be explained by a sequential process. Peaks, as they are familiar from ordinary ATI, should appear in the case of double ionization as well, but, to our knowledge, they have not been found either in experiments or calculations. It is not straightforward to measure the total-kinetic-energy spectrum because electrons from single ionization are more numerous by at least an order of magnitude, and because a correlated measurement of both electron energies is necessary. Restricted information about the electron correlation was obtained by measuring the recoil momenta of the doubly charged ions [8]. The recoil-ion momentum P balances the sum of the final electron momenta, $P=-(p_1+p_2)$, since the absorption of photons changes the total momentum of the system by only a negligible amount. Very recently, the full momentum correlation between the two electrons was determined by measuring recoil-ion momentum and electron momentum coincidently [9]. Wavelengths around 800 nm were used in these experiments. The corresponding photon energy is 1.55 eV and the experimental resolution did not allow the observation of any structures reminiscent of ATI peaks in the spectra. In a similar study [10], the single-electron energy distribution for double ionization was recently measured. Here, the number of recorded events was too low to resolve a peak structure. Besides that, it is not clear if the single-electron distribution should have peaks separated by the photon energy, because the total energy is shared by the two electrons and the energy of the second electron was not measured.

In this paper, we show numerically that laser pulses in the visible and ultraviolet produce distinct peaks in the double-ionization photoelectron spectra. Therefore, the experimental detection of such above-threshold double-ionization (ATDI) peaks should be possible. Even if we have experimental access only to the recoil-ion momentum spectrum, information about the peak structure in the full two-electron spectrum can be retrieved, as we will demonstrate below. This finding is highly nontrivial since the recoil-ion spectrum depends crucially on how the energy is shared between the electrons. The existence of ATDI peaks in the total-energy spectra is expected, but it is not obvious under which conditions they can be observed. In a very strong laser pulse, e.g., the atom is rapidly ionized within a few optical cycles. The formation of ATI or ATDI peaks, however, can be understood as interference between contributions ejected at different times over many cycles and therefore will not be observed for too short or too intense pulses.

The nonperturbative numerical solution of the full time-dependent two-electron Schrödinger equation in three dimensions (3D) [11] is very demanding and has been achieved so far only for small wavelengths, mainly in the ultraviolet range. The calculation of photoelectron energy spectra requires sufficiently dense continuum states (or, in other words, a large grid) and is therefore even more involved than the calculation of ionization probabilities. To demonstrate the existence of ATDI peaks, we therefore use the familiar one-dimensional model of a two-electron atom with soft Coulomb interactions [12], subject to an electric field $\mathcal{E}(t)\sin\omega t$. The time-dependent Schrödinger equation, in atomic units, for the two-electron wave function $\Psi(z_1,z_2,t)$,

$$i\frac{\partial\Psi}{\partial t}(z_1,z_2,t)=\left[\frac{p_1^2}{2}+\frac{p_2^2}{2}+(p_1+p_2)A(t)-\frac{2}{\sqrt{z_1^2+1}}-\frac{2}{\sqrt{z_2^2+1}}+\frac{1}{\sqrt{(z_1-z_2)^2+1}}\right]\Psi(z_1,z_2,t), \tag{1}$$

with $A(t)=-\int_0^t\mathcal{E}(t')\sin\omega t'dt'$, is solved numerically by means of the split-operator method [13]. As described in previous work [15], the configuration space spanned by the co-

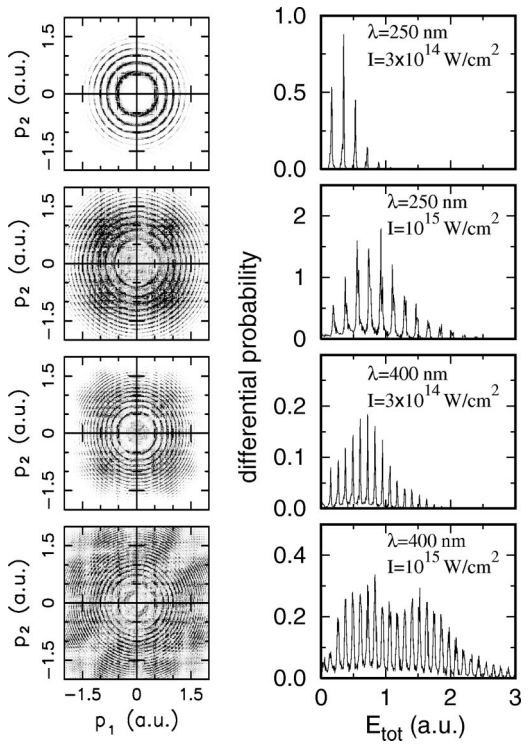

FIG. 1. Left: Two-electron momentum distributions for double ionization by laser pulses with wavelengths and intensities as indicated in the panels on the right-hand side. Right: Photoelectron total-kinetic-energy spectra for double ionization by laser pulses with wavelengths and intensities as indicated.

ordinates z_1, z_2 is divided into an inner region corresponding to the neutral atom ($|z_1|, |z_2| < a$) and two outer regions corresponding to single ionization ($|z_1| < a$, $|z_2| \geqslant a$ or $|z_1| \geqslant a$, $|z_2| < a$) and double ionization ($|z_1|, |z_2| \geqslant a$), respectively. In the outer parts, the electron-electron interaction is neglected, as well as the interaction between the nucleus and the far-away electrons. At the end of the propagation, the wave function in the double-ionization region yields the momentum and energy distributions that we present in the following.

Figure 1 shows the two-electron momentum distributions and the total-kinetic-energy spectra after the action of laser pulses with a duration of 20 fs. The field is switched on and off using 5 fs linear ramps. The most striking features of the momentum distributions are concentric circles, which are most pronounced at short wavelength and low intensity. Since the total kinetic energy is given by $E_{\mathrm{tot}} = p_1^2/2 + p_2^2/2$, these rings are lines of constant energy. The energy spectra on the right-hand side of Fig. 1 are obtained by integration of the momentum distributions. They consist of well-defined peaks that are in obvious correspondence to the rings of constant energy. In each case, the separation between adjacent peaks is constant throughout the spectrum and equals the photon energy.

In Fig. 2, the energy spectra for 250-nm pulses of three different laser intensities are plotted. Apparently, the peaks shift towards lower energy with increasing intensity. This is due to the fact that the oscillating electric field shifts the

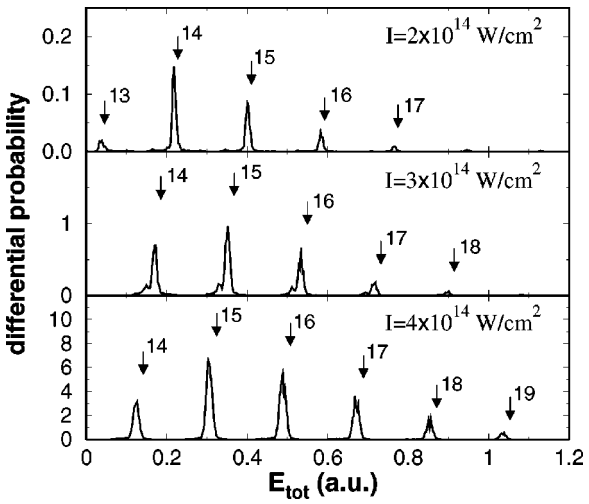

FIG. 2. Photoelectron total-kinetic-energy spectra for 250 nm pulses at various intensities. The arrows point to the peak energies expected from Eq. (2) for the given number of absorbed photons.

energy of the continuum states and thereby increases the ionization barrier. Analogous to ordinary short-pulse ATI, the position of the peaks can be approximately calculated as

$$E_n = n\hbar\omega - (I_p^{(2)} + 2U_p), \tag{2}$$

where n is the number of absorbed photons, $I_p^{(2)}$ is the double-ionization potential, and $U_p = \mathcal{E}^2/(4\omega^2)$ is the ponderomotive potential (which we evaluate at the peak amplitude). The increase in the ionization threshold amounts to U_p *per electron*. Hence the term $I_p^{(2)} + 2U_p$ appears, as opposed to ordinary ATI, where we have $I_p^{(1)} + U_p$. In Eq. (2), it is assumed that the ac Stark shift of the ground state is negligible. The energies predicted by Eq. (2) are indicated by arrows in Fig. 2; they give a good estimate for the peak energies. The number of absorbed photons is specified for each arrow. Using Floquet theory [14], we have calculated the quasi-ground-state energies and have confirmed that the small discrepancy is indeed due to the ac shift of the ground state: The ac shifts corresponding to the laser parameters of Fig. 2 are 0.0096 a.u. for 2×10^{14} W/cm^2, 0.014 a.u. for 3×10^{14} W/cm^2, and 0.025 a.u. for 4×10^{14} W/cm^2. The differences between the numerical peak energies and Eq. (2) are, on average, 0.009 a.u., 0.015 a.u., and 0.020 a.u., respectively. The very small remaining discrepancies are due to contributions from the leading and falling edge of the pulse where the intensity is below its peak value, or due to small numerical errors. The substructures in Fig. 2 come from laser-induced resonances giving rise to an additional series of peaks, also separated by the photon energy. This can be confirmed by inspection of the corresponding Floquet spectra.

We now turn our attention to the distribution of recoil-ion momenta (Fig. 3), because these can be measured with much less effort than the full correlated two-electron spectra [16]. As $P = -(p_1 + p_2)$, the recoil-ion momentum spectrum is calculated by integration of the two-electron momentum distribution. Again, we find a pronounced peak structure, at least in the case of small wavelength and intensity. However,

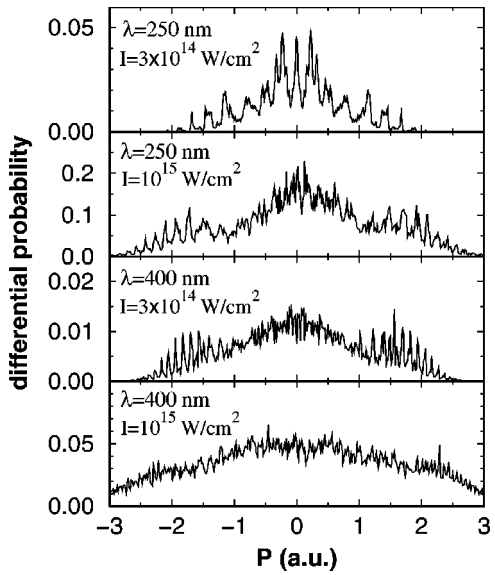

FIG. 3. Recoil-ion momentum distributions of doubly charged ions.

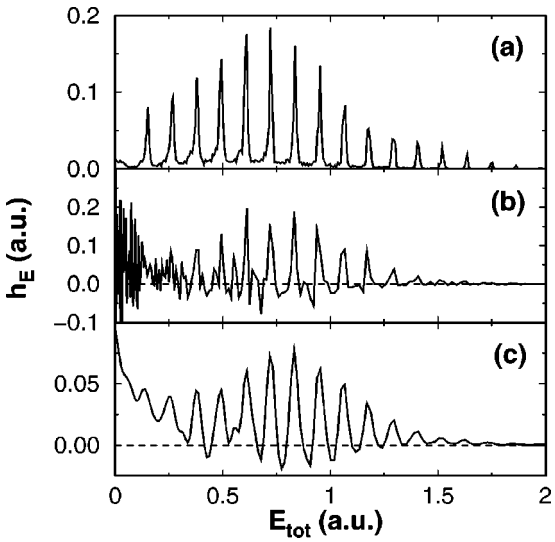

FIG. 5. Reconstruction of the total-kinetic-energy spectrum from the recoil-ion momentum distribution for a 400 nm pulse with intensity 3×10^{14} W/cm^2: (a) exact spectrum, (b) spectrum from solution of Eq. (3), (c) smoothed version of spectrum (b).

only part of these peaks is due to the ring structure in Fig. 1, and the relation is somewhat indirect. It is easily verified that in the region of large absolute values of P, the separation between two adjacent peaks corresponds to the photon energy $\hbar\omega$ if we calculate the energy as $E_{\rm tot}=P^2/4$. The reason for this behavior is obvious if only one circle of Fig. 1 with energy $E_{\rm tot}$ is considered, as is schematically shown in Fig. 4. The integration that leads from the two-electron momentum distribution (shown as the upper part of Fig. 4) to the P distribution (lower part of Fig. 4) is along the lines where p_1+p_2 is constant, i.e., along vertical lines in Fig. 4. A single ring with energy $E_{\rm tot}$ in the (p_1,p_2) plane gives rise to a distribution over P with two peaks and sharp cutoffs at the lower und upper ends, because the value of the vertical line integral is largest when the integration is along a tangent to the circle. In this case, we have $p_1=p_2=\pm\sqrt{E_{\rm tot}}$. Consequently, the peaks are located at $\pm P_{\rm max}=\pm2\sqrt{E_{\rm tot}}$, in agreement with the above result. The structures in the inner region of the P distributions originate from structures *within* the rings, mainly within the innermost ring. For 400 nm and 10^{15} W/cm^2, the calculation does not resolve the ATDI peaks even though the spacing must be the same as in the case of 3×10^{14} W/cm^2. The reason is twofold: (i) The outer ATDI rings (left-hand side of Fig. 1) have a more pronounced substructure, and (ii) the peaks in the energy spectrum (right-hand side of Fig. 1) are broadened due to pulse-shape effects (contributions of various intensities while the laser is switched on and off.)

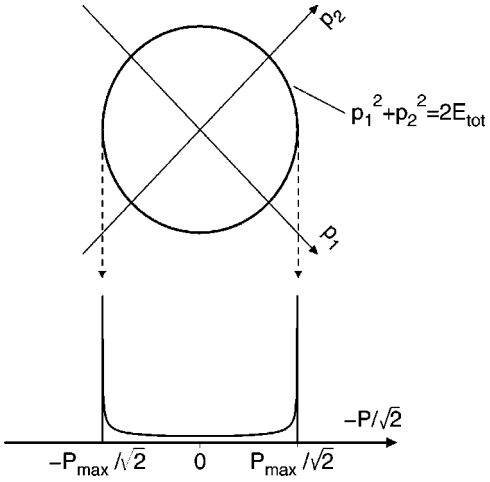

FIG. 4. Visualization of the appearance of peaks in the recoil-ion momentum distribution.

In general, the electron total-kinetic-energy spectrum cannot be retrieved from the recoil-ion spectrum because information is lost in the integration procedure. However, under some reasonable assumptions, such a reconstruction should be possible. To that end, we introduce a function $h(E,\phi)$ that is the distribution of the total energy E and the "angle" ϕ, which is defined by $\tan\phi=p_2/p_1$. Under the assumption that $h(E,\phi)$ is a product of an energy distribution and an angular distribution, $h(E,\phi)=h_E(E)h_\phi(\phi)$, and that the spectra have forward/backward symmetry $h_\phi(\phi)=h_\phi(3\pi/2-\phi)$, we calculate the recoil-ion momentum distribution $R(P)$ as

$$R(P)=\int_{P^2/4}^{\infty}h_E(E)h_\phi\left(\arctan\frac{P+2f(E,P)}{P-2f(E,P)}\right)\times\frac{dE}{f(E,P)},\tag{3}$$

where $f(E,P)=\sqrt{E-(P^2/4)}$. We assume further that the energy spectrum does not extend up to infinity so that the upper limit of the integral can be replaced by a finite value $E_{\rm max}$. Then, for given functions $R(P)$ and $h_\phi(\phi)$, Eq. (3) is a Volterra integral equation for $h_E(E)$ and can readily be solved numerically [17]. Figure 1 shows that the two-electron distributions are not very anisotropic in the (p_1,p_2) plane. (This is different for long wavelengths around 800 nm [9,15].) Therefore, we simply use a constant function h_ϕ

$=1/(2\pi)$ in this paper, but the method is not restricted to a particular choice of h_ϕ. There are some rapidly varying substructures within the rings, which should in principle enter the function h_ϕ. However, the effect of these substructures can be greatly reduced by smoothing the resulting energy distribution $h_E(E)$, which is much more efficient than trying to reproduce the complicated ϕ dependence. The result of the procedure is presented in Fig. 5 for the example of a 400 nm pulse with intensity 3×10^{14} W/cm^2. The upper panel shows the exact calculated energy spectrum, and panel (b) shows the spectrum that is reconstructed from the recoil-ion momentum distribution by the solution of Eq. (3). We find peaks at the correct positions, but also we find a rapidly oscillating substructure and negative values of h_E. The oscillations can be suppressed by convolution with a Gaussian distribution of 0.04 a.u. width (full width at half maximum). Thus we arrive at the spectrum in panel (c). Considering the crudeness of the approximation, the agreement with the exact spectrum is excellent: The peak positions are correct, and the envelope is well reproduced except for small energies lower than 0.5 a.u.

Equation (3) has been derived for the 1D model, knowing that the photoelectrons are preferentially ejected along the laser polarization: Ref. [18] indicates that the angle between the two electrons deviates not more than $\pi/6$ from zero or π. Together with the fact that the recoil-ion momentum is strongly aligned with the polarization axis [8,19], we conclude that for nearly equal moduli of the electron momenta, the angle of electron emission is typically less than $\pi/12$, reducing the peak positions in the recoil-ion spectra by at most a factor of $\cos(\pi/12)\approx0.97$. Thus we expect that the reconstruction procedure can be applied to experimental spectra and will be helpful in the detection of the ATDI peaks.

To summarize, we have demonstrated the existence of ATDI peaks for a variety of laser parameters. The peaks appear not only in the photoelectron total-energy spectra, but also in the recoil-ion momentum distributions, which can be measured much more easily. We have proposed a numerical method to approximately extract the former from the latter.

This work was supported by the Deutsche Forschungsgemeinschaft.

[1] P. Agostini, F. Fabre, G. Mainfray, G. Petite, and N.K. Rahman, Phys. Rev. Lett. **42**, 1127 (1979).
[2] J.H. Eberly, J. Javanainen, and K. Rzążewski, Phys. Rep. **204**, 331 (1991).
[3] G.G. Paulus *et al.*, Phys. Rev. Lett. **72**, 2851 (1994).
[4] G.G. Paulus *et al.*, Phys. Rev. Lett. **80**, 484 (1998).
[5] H.G. Muller, Laser Phys. **9**, 138 (1999); Phys. Rev. Lett. **83**, 3158 (1999).
[6] D.N. Fittinghoff, P.R. Bolton, B. Chang, and K.C. Kulander, Phys. Rev. Lett. **69**, 2642 (1992).
[7] B. Walker *et al.*, Phys. Rev. Lett. **73**, 1227 (1994).
[8] Th. Weber *et al.*, Phys. Rev. Lett. **84**, 443 (2000); R. Moshammer *et al., ibid.* **84**, 447 (2000); Th. Weber *et al.*, J. Phys. B **33**, L127 (2000).
[9] Th. Weber *et al.*, Nature (London) **405**, 658 (2000).
[10] B. Witzel, N.A. Papadogiannis, and D. Charalambidis, Phys. Rev. Lett. **85**, 2268 (2000).
[11] J. Zhang and P. Lambropoulos, J. Phys. B **28**, L101 (1995); A. Scrinzi and B. Piraux, Phys. Rev. A **56**, R13 (1997); D. Dundas, K.T. Taylor, J.S. Parker, and E.S. Smyth, J. Phys. B **32**, L231 (1999).
[12] R. Grobe and J.H. Eberly, Phys. Rev. A **48**, 4664 (1993).
[13] M.D. Feit, J.A. Fleck, Jr., and A. Steiger, J. Comput. Phys. **47**, 412 (1982).
[14] J.H. Shirley, Phys. Rev. **138**, B979 (1965).
[15] M. Lein, E.K.U. Gross, and V. Engel, Phys. Rev. Lett. **85**, 4707 (2000).
[16] R. Dörner (private communication).
[17] W. H. Press, S. A. Teukolsky, W. T. Vetterling, and B. P. Flannery, *Numerical Recipes* (Cambridge University Press, Cambridge, 1992).
[18] K.T. Taylor *et al.*, Laser Phys. **9**, 98 (1999).
[19] A. Becker and F.H.M. Faisal, Phys. Rev. Lett. **84**, 3546 (2000).